R. Ra'e Ga
Curitiba, v.46, n. 3, p. 07 - 19, Set/2019

DOI: 10.5380/raega
eISSN:2177-2738

RA'EGA
O ESPAÇO GEOGRÁFICO EM ANÁLISE

# DYNAMICS OF HEAT FLUXES BY BOWEN AND MATMNXFLX AND NOAH FLDAS PRODUCTS IN THE PANTANAL OF MATO GROSSO - BRAZIL

# DINÂMICA DOS FLUXOS DE CALOR POR BOWEN E PRODUTOS MATMNXFLX E FLDAS NOAH NO PANTANAL MATO-GROSSENSE

Leilane Gomes Duarte [1], Kelly Souza Romera [1], Marlus Sabino [1], Leone Francisco Amorim Curado [1], Rafael da Silva Palácios [1], José de Souza Nogueira [1]

**ABSTRACT**
This paper aimed to analyze the dynamics of the energy budget components: latent heat flux (LE), sensible heat flux (H) and soil heat flux (G), in the Mato Grosso Pantanal. The estimates of LE, H, and G were obtained by the Bowen ratio methods, using data from the micrometeorological tower located in the Baía das Pedras Park of SESC-Pantanal Ecological Resort, for the years 2011 to 2013. The normality of the variables Rn, LE, H and G, were tested by Kolmogorov-Smirnov test at 5% significance, and the seasonal differences of the fluxes were verified by the Kruskal-Wallis test, α = 0.05. LE and H data from the remote sensing products MATMNXFLX and FLDAS_NOAH of the MERRA model was also acquired, and their comparison with the tower data was performed by the statistics of Spearman correlation (r), Mean Absolute Error (MAE), Root Mean Squared Erro (RMSE), bias, and Willmott's Concordance Index (d). It was observed that most of the available energy is used for evapotranspiration (latent heat), followed by sensible heat and soil heat flux. In the rainy season there is an increase in the partition of LE and G and reduction of H. Only the estimates of LE of MATMNXFLX and FLDAS_NOAH products correlate with the data observed in the meteorological tower. It is concluded that the energy partitions have a seasonal behavior and that the MATMNXFLX and FLDAS_NOAH products, after being calibrated, can be used to estimate LE in the Mato Grosso Pantanal.

**Keywords:** Bowen's Ratio; net radiation; Wetlands; Seasonality; Remote Sensing.

**RESUMO**
Analisou-se a dinâmica das componentes do saldo de radiação (Rn) destinadas aos fluxos de calor latente (LE), sensível (H) e fluxo de calor no solo (G) no Pantanal Mato-Grossense. As estimativas do LE, H e G foram obtidas pelos métodos da razão de Bowen por meio de dados da torre micrometeorológica localizada no Parque Baía das Pedras da Estância Ecológica SESC-Pantanal, durante os anos de 2011 a 2013. Foram testadas a normalidade das variáveis Rn, LE, H e G, por meio do teste de Kolmogorov-Smirnov a 5% de significância, e a diferença sazonal dos fluxos foi verificada pelo teste de Kruskal-Wallis, α= 0.05. Foram ainda adquiridos dados de LE e H dos produtos de sensoriamento remoto MATMNXFLX e FLDAS NOAH do modelo MERRA e sua comparação com os dados da torre foi realizado pelas estatística da Correlação de Spearman (r), Erro Médio Absoluto (MAE), Raiz do Erro Quadrático Médio (RMSE), viés e Índice de Concordância de Willmott (d). Observou-se que a maior parte da energia disponível é utilizada para a evapotranspiração (calor latente), seguida do calor sensível e do fluxo de calor no solo. No período chuvoso há aumento da partição do LE e G e redução do H. Apenas as estimativas de LE dos produtos MATMNXFLX e FLDAS_NOAH apresentam correlação com os dados observados na torre meteorológica. Conclui-se que as partições de energia apresentam comportamento sazonal e que os produtos MATMNXFLX e FLDAS_NOAH, após calibrados, podem ser utilizados na estimativa do LE nas condições do Pantanal Mato-Grossense.

**Palavras chave:** Razão de Bowen; Net Radiation; Áreas Úmidas; Sazonalidade; Sensoriamento Remoto.

Recebido em: 20/05/2019
Aceito em: 19/07/2019

[1] *University of the State of Mato Grosso (Câmpus Cuiabá). emails: {leilane, kellyromera}@fisica.ufmt.br, {marlussabino, leonecurado, rafael.pgfa, paranagueira}@gmail.com.*

**DYNAMICS OF HEAT FLUXES BY BOWEN AND MATMNXFLX AND NOAH FLDAS PRODUCTS IN THE PANTANAL OF MATO GROSSO**

## 1. INTRODUCTION

The Pantanal biome is an intermittently flooded plain located in South America between Brazil, Paraguay, and Bolivia, being considered as one of the largest continuous wetlands on the planet. In Brazil, it occupies about 150,355 km2 of the national territory located between the States of Mato Grosso and Mato Grosso do Sul (IBGE, 2004; DA SILVA e DE MOURA ABDON 1998, p.1703-1711).

A particular feature of the Pantanal region is the seasonal variation of soil surface water level, which classifies the Pantanal into the category of temporarily flooded area. The seasonal tendency of rainfall in tropical and subtropical regions (DA SILVA et al., 2018 p. 178-182) associated with topography and the clayey soil of the place are the main factors for the occurrence of floods in the rainy season (November to April) and water recess in the drought season (May to September) (CURADO et al., 2011, p.167; MACHADO et al., 2016, p.82-91).

The flood dynamics of the Pantanal makes this region especially important for the understanding of the variations of the energy flows in seasonally flooded areas since the presence of water in the environment is one of the main contributors in determining the partitioning of energy between the surface and the atmosphere (CURADO et al., 2011, p.167).

In general, the energy available in the medium from the net radiation is converted to latent heat flux (LE), which includes the evapotranspiration process; sensible heat (H) used in air heating; and soil heating flux (G). When a change occurs in the partitions of the LE and H flows, the characteristics of the microclimate are affected, therefore, being aware of the energy budget on vegetated surfaces is extremely important to determine water losses and biomass accumulation (FOLEY et al., 2003, p.38-44; RODRIGUES et al., 2011, p.165-175).

The microclimatic variables and the energy flux components were obtained in a punctual way from surface data, making it difficult to understand the variation of the components in larger scales. In this way, the development of technology of environmental satellites, through mathematical models with acceptable accuracy enabled the obtaining of meteorological information in large areas (ARAUJO et al., 2017, p. 434).

In this context, the latent and sensible heat fluxes estimates provided by the MATMNXFLX and FLDAS NOAH products have been showing to be an alternative for large-scale studies of variations of the components of the energy budget in places with low availability of surface data such as the Pantanal.

The latent and sensible heat flux estimates of the MATMNXFLX and NOAH FLDAS products are obtained from the Modern-Era Retrospective Analysis for Research and Applications (MERRA) model administered and made available by NASA. The surface flows in MERRA are the result of the parameterization of complex physical processes of molecular and turbulent diffusion, boundary layer structure and dynamic processes, being able to produce consistent estimates of turbulent and radiative fluxes (ROBERTS et al., 2012, p. 836).

The advantages of the flow estimates of MATMNXFLX and NOAH FLDAS products are related to both the global satellites coverage and series extension, with data since 1979 and 1982 for MATMNXFLX and NOAH FLDAS, respectively. However, the estimates obtained by sensing require comparisons and calibrations with locally obtained data before being applied effectively.

Thus, this study aims to analyze the seasonal dynamics of latent heat fluxes (LE), sensible heat (H) and soil heat flux (G) obtained by Bowen method, as well as, compare the in-situ flux estimative with the remote sensing products MATMNXFLX and NOAH FLDAS in the Mato Grosso Pantanal.

## 2. MATERIAL AND METHODS

### 2.1. Location of Experimental Area

The study area is located at the Advanced Research Center of the Federal University of Mato Grosso, located in the Baía das Pedras Park of SESC-Pantanal Ecological Estancia, in the North region of Pantanal (16º29'52 "S and 56º24'47" W) in the city of Poconé (Mato Grosso State – Brazil), approximately 160 km from the capital Cuiabá, MT.

The predominant vegetation in the study area is known as pombeiral. The soils, which are in dominance of clayey hydromorphic, are of sedimentary origin; the topography is flat and seasonal floods occur in the rainy season (MACHADO et al., 2015, p.81-90; FANTIN-CRUZ et al., 2010, p. 31-38). According to the classification of Köppen, the climate of the region is Aw, being warm and humid in summer, which is the rainy season, and drought in winter. The region presents average annual precipitation of 1400 mm with drought from May to October (NUNES DA CUNHA; JUNK, 2001, p. 63-70) and average annual temperature of 26.1°C (BIUDES et al., 2015, p. 112-124).

### 2.2. Instrumentation

The data from net radiation, soil heat flux, temperature gradients and relative humidity used in this study was obtained at the micrometeorological tower installed at the study site. Data was collected between June 2011 and October 2013. The rainy season comprehends the months from November to April and the drought season the months from May to November.

The net radiation was measured by a net radiometer (Net Radiometer, Kipp & Zonen Delft, Inc. Holland) and the heat fluxes of soil were obtained by soil heat flux sensors installed at 1cm depth. The temperature and humidity gradients were acquired by thermohygrometers (model HMP45C) installed at 21, 40 and 30 m above the ground. Data collected by the equipment was processed and stored in a CR 10X datalogger, Campbell Scientific, Inc.

The measurements of the soil heat flux, the temperature and humidity gradients were used to calculate the Bowen Ratio and obtain partition of the latent and sensible heat fluxes in the energy budget (BOWEN, 1926).

### 2.3. Energy Budget Estimate Using the Bowen Ratio Method

In the estimation of heat fluxes on a surface, the energy budget can be represented in a simplified form as the sum of the latent heat (LE), the sensible heat (H) and the heat soil flux (G) (Equation 1).

Equation 1

$$Rn = G + H + \mathrm{LE}$$

In which: Rn is net energy budget by the radiometer balance ($Wm^{-2}$); G is the soil heat flux obtained by the flow meter ($Wm^{-2}$); LE is the latent heat ($Wm^{-2}$); H is the sensible heat ($Wm^{-2}$).

From Equation 1, the Bowen ratio method (β) is used to estimate the components LE and H of the net radiation, since the Bowen ratio is the ratio between the sensible heat (H) and heat fluxes latent (LE), according to equation 2:

Equation 2

$$\beta = \frac{H}{LE}$$

Considering an average time (t) between 20-60 min, one can consider the occurrence of empirical relations between energy flows and vertical gradients of temperature and vapor pressure in air, according to Equations 3 and 4:

Equation 3

$$LE = \frac{-\rho C_p}{\gamma} K_w \frac{\Delta e}{\Delta z}$$

Equation 4

$$H = -\rho C_p K_s \frac{\Delta t}{\Delta z}$$

In which: Cp is the value of the specific heat of air at constant pressure (1010 J $kg^{-1}$ $ºC^{-1}$); ρ is the local atmospheric pressure (kPa); γ is the psychrometric constant (kPa $ºC^{-1}$); Δt is the temperature difference between two levels of height Δz (ºC); Δe is the atmospheric vapor pressure difference between two levels of height Δz (kPa); Δz is the height difference in the atmospheric profile in which the temperature and/or pressure equipment (m); and Ks and Kw are the coefficients of turbulent diffusivity ($m^2 s^{-1}$).

According to Verma et al. (1978), the turbulent diffusivity coefficients Ks and Kw are equal, so by applying Equations 3 and 4 in Equation 2, the Bowen ratio can be obtained according to Equation 5:

Equation 5

$$\beta = \gamma \frac{\Delta t}{\Delta e}$$

The value of the psychrometric constant is given by the relation between the specific heat of the air (Cp), the atmospheric pressure (ρ) and the latent heat of vaporization (L) (kJ kg-1) (Equation 6).

Equation 6

$$\gamma = \frac{(C_p p)}{0{,}622.L}$$

The atmospheric vapor pressure is obtained by means of the relative humidity (UR) (Equation 7), due to the relation between the current water vapor pressure (e) and the water vapor saturation pressure (s) given in function (Equation 8).

Equation 7

$$UR = \frac{e}{e_s} 100$$

Equation 8

$$e_s = 0{,}6108 e^{\left(\frac{17{,}27T}{T+237.3}\right)}$$

After obtaining the Bowen ratio (Equation 5), applying Equation 2 in Equation 1, the sensible (Equation 9) and heat fluxes latent heat (Equations 10) are acquired.

Equation 9

$$H = (Rn - G) \frac{\beta}{\beta + 1}$$

Equation 10

$$LE = \frac{(Rn - G)}{\beta + 1}$$

In order to avoid physical inconsistencies in the estimates made by the Bowen (β) Ratio Method, Perez et al. (1999, p.141-150) describe a series of criteria that should be used for the correct determination of fluxes estimated by Bowen's ratio for heat flux (LE) and sensible heat (H). According to the authors, it is suggested that values that do not respect these conditions should be discarded. Therefore, in this study it was only maintained data consistent with the criteria presented in Table 1.

| Available energy | The atmospheric vapor pressure difference | Bowen ratio | Heat flows |
|---|---|---|---|
| $R_n - G > 0$ | Δe > 0 | -1 < β ≤ 0 | LE > 0 e H ≤ 0 |
| | | β > 0 | LE > 0 e H > 0 |
| | Δe < 0 | β < -1 | LE < 0 e H > 0 |
| $R_n - G < 0$ | Δe > 0 | β < -1 | LE > 0 e H < 0 |
| | Δe < 0 | -1 < β ≤ 0 | LE < 0 e H ≥ 0 |
| | | β > 0 | LE < 0 e H < 0 |

**Table 1 -** Conditions to be satisfied by the Bowen method under non-advective conditions for reliable and consistent data. Rn – net radiation; G - soil heat flux Δe - the vapor pressure difference between lower and upper measurement levels;LE and H latent and sensible heat flux, respectively. Adapted from Perez et al. (1999, p.141-150).

The normal distributions of the variables from the meteorological tower and estimated by Bowen's method (Rn, LE, H and G) were then tested by means of the Kolmogorov-Smirnov test at 5% significance and the mean values and range of confidence of 95% of each variable, by the bootstrapping method of 1000 iterations of the random resampling with substitution (EFRON; TIBSHIRANI, 1993). The difference of flows in relation to seasonality was also tested by the Kruskal-Wallis test, α = 0.05, for variables with non-normal distribution.

### 2.4. Comparison of the flows obtained by Bowen and the sensing products

The results of latent and sensible heat flux obtained by the Bowen method were further compared with the measures of LE and H estimated by the product MATMNXFLX and FLDAS NOAH obtained from the collection of Modern-Era Retrospective analysis for Research and Applications (MERRA) filed at the Data and Information Services Center of Goddard Earth Sciences (GES DISC) (http://disc.sci.gsfc.nasa.gov/).

The MATMNXFLX product is available in monthly time resolution and spatial resolution of 0.5 ° x 0.677 °. The NOAH FLDAS product, in turn, presents a monthly and spatial resolution of 0.1 ° x 0.1 °. The detailed documentation on the data assimilation processes of the MERRA model is made available by Rienecker et al. (2011, pp. 3624-3648), Mcnally et al. (2017, p.170012), and Bloom et al. (2005, p.779-787).

The comparison of MATMNXFLX and NOAH FLDAS data to local conditions was performed by linear regressions between the data estimated by the satellite and observed in the micrometeorological tower. The regression models were evaluated by means of the coefficient of determination and p-value.

The regression models considered satisfactory (p-valor < 0.05) were then subjected to performance analysis using the Spearman correlation coefficient (p); mean absolute error (MAE); root means square error (RMSE); bias; bias% and Willmott's concordance index, obtained, respectively, by Equations 11 to 16.

Equation 11

$$p = \frac{\sum_{i=1}^{n}(o_i - ó)(p_i - ṕ)}{\sqrt{[\sum_{n=1}^{n}(o_i - ó)^2][\sum_{n=1}^{n}(p_i - ṕ)^2]}}$$

Equation 12

$$MAE = \frac{1}{N}\sum_{i=1}^{N}|O_i - P_i|$$

Equation 13

$$RMSE = \sqrt{\frac{1}{N}\sum_{i=1}^{N}(O_i - P_i)}$$

Equation 14

$$Bias = \frac{1}{N}\sum_{i=1}^{N}(O_i - P_i)$$

Equation 15

$$Bias(\%) = \frac{\sum_{i=1}^{n}(O_i - P_i)}{\sum_{i=1}^{n} P_i}$$

Equation 16

$$d = 1 - \left[\frac{\sum_{i=1}^{N}(P_i - O_i)^2}{\sum_{i=1}^{N}(|P_i - O| + |O_i - O|)^2}\right]$$

In which, Pi are the estimated values; Oi is the observed values; N is the number of observations; $Ó$ is the arithmetic mean of the observed values; and $Ṕ$ is the arithmetic average of the estimated values.

## 3. RESULTS AND DISCUSSIONS

### 3.1. Temperature and Relative Humidity

The rainy season presented the highest air temperature values, about 27°C, while the drought season the lower, about 24°C. Nevertheless, in spite of the smaller averages, the drought season had a greater amplitude of the temperature with maximum and minimum between 15.1 and 33.6°C (2011); 13.9 and 33.6°C (2012), and 11.2 and 29.9°C (2013) (Figure1a).

Similar to temperature, relative humidity and net radiation (Rn) also presented seasonal behavior with higher values in the rainy season. The average monthly values of humidity ranged from 56 to 91% in the rainy season and 34 to 90% in the drought season (Figure 1a). The average Rn of the 2011/2012 rainy season was 9.05% higher than the values found for the drought season of 2011, as well as the average Rn of the rainy season 2012/2013 was 11.53% higher to the drought season of 2012. (Figure 1b).

In land use, there was the presence of Agriculture, Areas degraded by mining, Urban influence, Livestock contacts with different types of vegetation, Livestock with Presence of Secondary Vegetation, Silviculture, Secondary Vegetation and Water (Table 1). Such a variety of flora can be attributed to the occurrence of the biomes Amazônia, Cerrado and Pantanal (BRASIL, 2018).

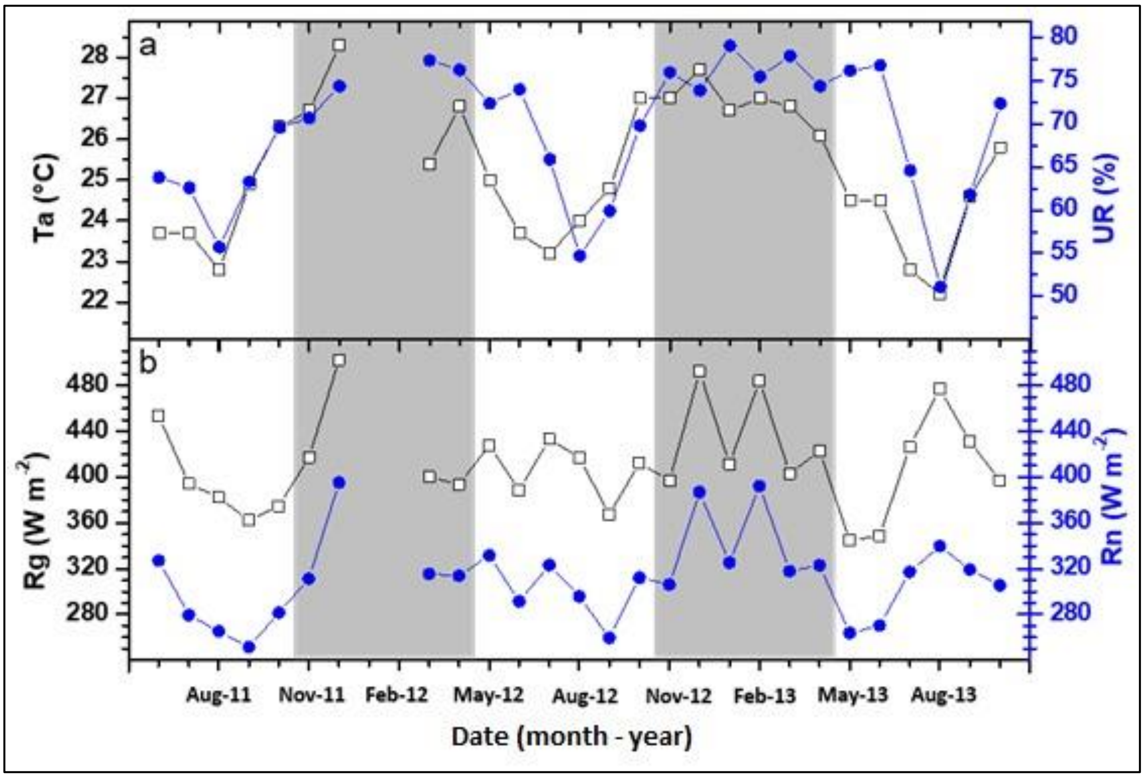


**Figure 1.** a) Monthly averages of air temperature (Ta) and relative air humidity (UR). b) Global radiation (Rg) and net radiation (Rn) in the season of rain (gray background) and drought (white background) from 2011 to 2013 for the Baía das Pedras region.

Higher temperature and humidity trends in the rainy season were also reported by Souza et al. (2013) in 13 meteorological stations in the state of Mato Grosso. In addition, the increase in the net radiation at this station was reported in the works of Curado et al. (2014, pp. 219-230) and Machado et al. (2016, pp. 82-91), which were carried out in Pantanal and Cerrado Mato Grosso biomes. The highest values of these climatic variables occur in the rainy months, since this season corresponds to the summer in the southern hemisphere and there is greater availability of radiation (VAREJÃO-SILVA, 2006, p.17).

The higher temperature and humidity in the rainy season also influenced the balance of radiation. Since the water vapor in the atmosphere presents great efficiency in the absorption of long waves, in this season, the highest energy use is allocated to the net radiation (SANTOS et al., 2013, p.72-88).

During the drought season, however, the highest burnings in the region occur increasing the number of particulate material present in the atmosphere. The presence of these aerosols, together with the low water vapor content, influence the incident solar, energy budget, causing reductions in the net radiation (CURADO et al., 2014, p. 219-230, MACHADO et al., 2016, p.82-91).

### 3.2. Seasonal Variation of Energy Budget Components

The seasonal means of the components of radiation fluxes are described in Table 2. None of the evaluated variables presented normal distribution by Kolmogorov-Smirnov test at 5%. Nonetheless, it was observed that there was a seasonal difference in the fluxes of the components of the net radiation by the Kruskal-Wallis test, $\alpha = 0.05$

It can be observed that the values destined to the component of the latent heat flux were higher than those of sensible heat flux in all evaluated periods. These results differ from those found by Rodrigues et al. (2014, p.1-13) in a study carried out in the Cerrado Biome, in which for the drought season there is a predominance of sensible heat flux. The higher LE values for the Pantanal in the drought season show that for the region, even without precipitation occurrence, no water restriction occured, thus maintaining the high rate of evapotranspiration.

| Season | Variable (W $m^{-2}$) | | | |
|---|---|---|---|---|
| | **Rn** | **LE** | **H** | **G** |
| Drought 2011 | 304.98 ± 17.52 b | 271.4 ± 16.95 b | 31.22 ± 2.77 a | 2.36 ± 0.75 ab |
| Rain 2011/12 | 335.32 ± 22.76 ab | 308.3 ± 22.01 ab | 23.48 ± 3.59 b | 3.55 ± 0.98 a |
| Drought 2012 | 301.69 ± 17.12 b | 267.64 ± 16.55 b | 32.28 ± 2.7 a | 1.78 ± 0.73 b |
| Rain 2012/13 | 340.98 ± 17.21 a | 314.71 ± 16.65 a | 23.28 ± 2.72 b | 2.99 ± 0.74 ab |

**Table 2 -** Mean and confidence limits of the net radiation (Rn) and the partitions of the Latent Heat (LE), Sensible Heat (H) and Soil Heat Flow (G) flows in the rainy and drought season of 2011 to 2013 for the Baía das Pedras region.

Averages followed by the same letter in the column do not differ from each other by the Kruskal-Wallis test ($P \leq 0.05$).

The monthly variations of the latent, sensible and soil heat fluxes are presented in Figure 2. The sensible heat flux showed a behavior contrary to that observed for latent heat flux, i.e., it is noted that the H decreased in the first months of rain and increased again in the months of drought season, reaching maximum values in the months of July and August and minimums in the months of February and March.

At the beginning of the rainy season the water availability of the environment increases, thus favoring the use of the available energy of the net radiation for the evapotranspiration processes. The LE becomes maximum in the month of February, since it corresponds to the month in which the water blade on the surface of the soil is maximum in the region of study and most of the available energy is used to evaporate the water in the surface flooded.

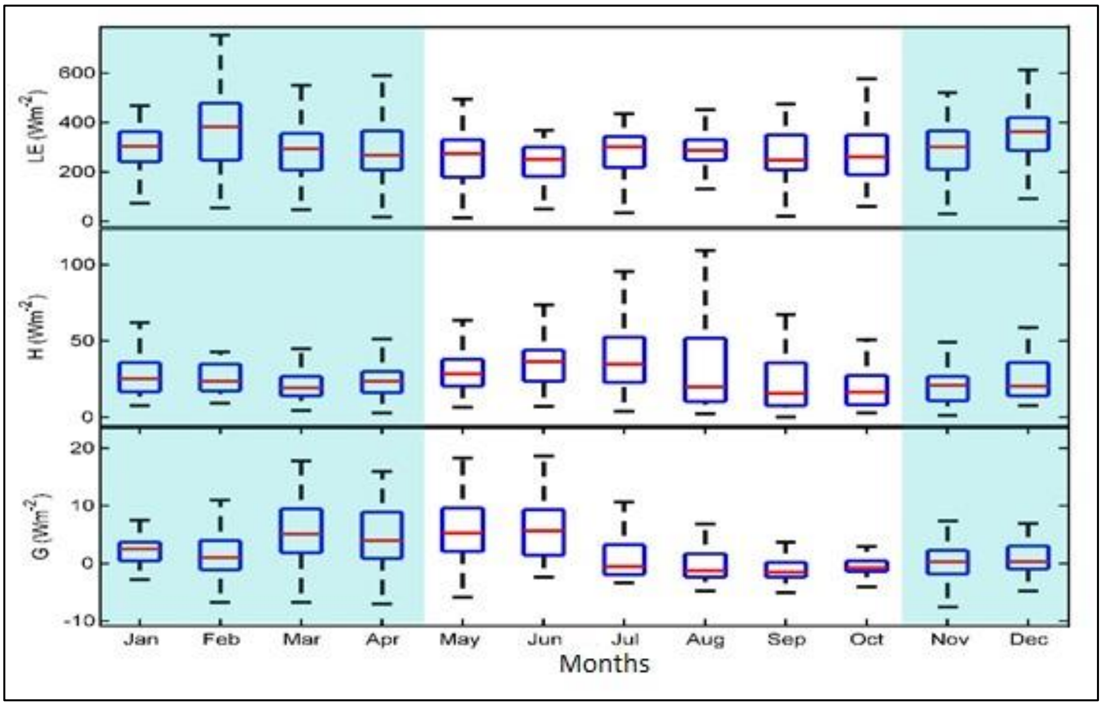


**Figure 2 -** Representation of variation latent heat (LE), sensible heat (H) and soil (G) rainfall in the rainy season (blue background) and drought (white background) for Baía das Pedras.

During the drought season, the water blade on the surface is reduced, decreasing the environment water availability. Under these conditions, as indicated by Bastable et al. (1993, pp. 783-796); Meinzer et al. (1999, p. 273-282); and Biudes et al. (2009, p. 135-143), the available energy of Rn is used for the soil heating, which directly warm up the adjacent air layer, causing an increase in the sensible heat flux, and, consequently, a decrease in the latent heat flux.

As a result, soil heat flux was lower in the months corresponding to the end of the drought season, showing an increase between November and February and reaching higher values between the months of March and June when the partition of energy in the soil remained practically constant. Therefore soil heat flow in the Pantanal region is directly influenced by floods.

The low values during the drought season are explained because the energy accumulated in the soil during the day is lost at night; since there is no radiation at night. thus, soil heat is used to warm the layers of air adjacent to the surface. In November, with the beginning of the rainy season, the water table starts to rise above the ground and it is observed increasing trends of G.

Upon receiving solar radiation, the water blade above the ground heats up, generating a vertical energy flow towards the flooded soil, warming it. Therefore, according to Burke et al. (1998, p. 31-51), the energy stored in the water blade continues to be transmitted to the soil during the night, so there is no loss of soil heat during flood periods.

In this way, seasonal floods are one of the important factors in variation partitions of net radiation energy in the Pantanal areas, being responsible, among others, for maintaining the high latent heat partition throughout the year and increasing the flow of heat in the soil.

### 3.3. Comparison of sensing products

The MATMNXFLX and NOAH FLDAS sensing products presented trends of underestimation of latent heat flux and overestimation of sensible heat flux, as can be observed in Figure 3.

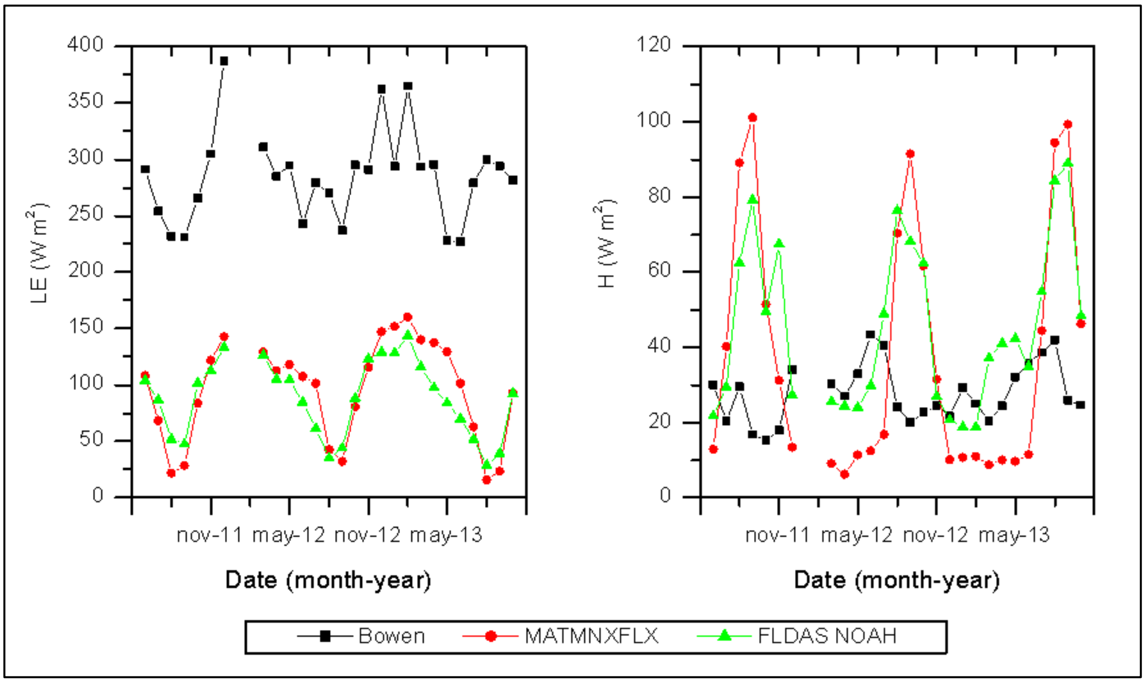


**Figure 3 -** Representation of the mean variation of the latent heat (LE) and sensible heat (H) fluxes obtained by Bowen's method and by the estimates of the remote sensing products MATMNXFLX and FLA NOAH for the Baía das Pedras region.

Similar trends were also found in the work of Roberts et al. (2012, p. 836), in which the latent heat flux is overestimated by the products of the MERRA model at 25 W m$^2$, for observed values of less than 50 W m$^2$, and can reach estimation errors in the order of 250 W m$^2$ for values observed above 150 W m$^2$. Roberts et al. (2012, p 836) also point out that for the sensible heat flux the products of MERRA model can be overestimated by approximately 50% for values lower than 210 W m$^2$.

Differences between values measured by satellites and observed fluxes are generally caused by the presence of vies in the acquisition of vertical gradients of humidity, temperature and, for MERRA model, mainly, wind velocity close to the surface (ROBERTS et al., 2012, p. 836). In addition, the Bowen method does a local estimate in peripheral areas of the micrometeorological tower, while the satellites estimate the flows of energy at a minimum area of approximately 74.12 km X 55.56 km. Thus, satellites estimative represent a mean value of flows in different surface characteristics, such as flooded areas, forest canopy, exposed soil, among others. The linear regressions obtained between the Bowen data and estimated by the sensing products are presented in Figure 4. For both products, only the latent heat flux data presented significant adjustment results (p-value <0.05), thus only the LE estimates of MATMNXFLX and FLA NOAH products were tested for calibration performance.

The performance analysis of the MATMNXFLX and NOAH FLDAS remote sensing products in the estimates of latent heat flux components values with the data obtained by the Bowen method before and after the application of regression adjustments are presented in Table 3. In this way, it is observed that the adjustment provided an improvement in the LE estimates, with a reduction of underestimation trends of -66.93% and -69.31% to 1.34% and 1.15%, respectively, in MATMNXFLX and FLDAS NOAH products.

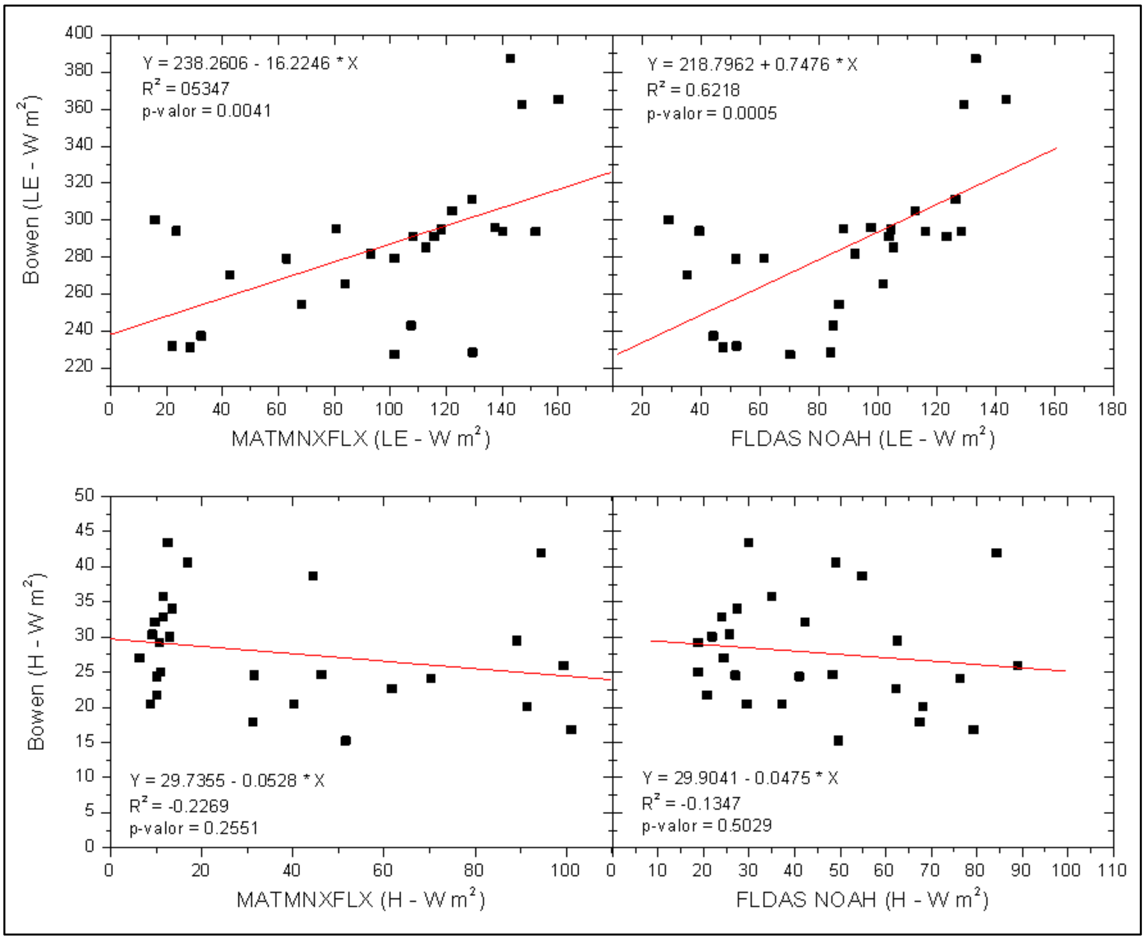


**Figure 4 -** Linear adjustments of the Latent Heat (LE) and Sensible Heat (H) fluxes obtained by the Bowen method and by the estimates of the remote sensing products MATMNXFLX and FLDAS NOAH for the Baía das Pedras region.

| Products | r | MAE ($W\ m^2\ s^{-1}$) | RSME ($W\ m^2\ s^{-1}$) | Bias ($W\ m^2\ s^{-1}$) | Bias (%) | d |
|---|---|---|---|---|---|---|
| Satellite products without Calibration | | | | | | |
| MATMNXFLX (LE) | 0.5244 | 189.48 | 193.72 | -189.48 | -66.93 | 0.2486 |
| FLDAS NOAH (LE) | 0.6105 | 196.45 | 199.08 | -196.44 | -69.31 | 0.2421 |
| Calibrated satellite products | | | | | | |
| MATMNXFLX (LE) | 0.5244 | 24.68 | 82.9 | 0.0005 | 1.34 | 0.6564 |
| FLDAS NOAH (LE) | 0.6105 | 25.06 | 76.8 | 0.0003 | 1.15 | 0.7302 |

**Table 3 -** Spearman (r) Correlation, Mean Absolute Error (MAE), Root Mean Square Error (RMSE) and Willmott's Concordance Index (d).

Roberts et al. (2012, p. 836) and Gonçalves (2016, p. 92) working with products of MERRA and NOAH models, also did not obtain good fits of the heat fluxes, although, both authors, also obtained satisfactory results in the calibration of the latent heat flux. The low correlation between the data observed in the towers and estimated by the satellites can be related to a large number of both physical processes involved and occurrence of uncertainties in the modeling of these processes as a measurement: errors, simplifications of models, initial conditions and representativeness of parameter values (GONÇALVES, 2016. p. 92).

It should be noted that the analysis of the dynamics of the energy budget components, as well as the adjustment regressions of the MATMNXFLX and FLDAS NOAH products on latent heat estimates are part of partial results and it is necessary to increase the time of the data series in order to characterize more confidently the variations in flows and estimates of satellites.

## 4. CONCLUSIONS

The components of the energy budget: net radiation (Rn), latent heat flux (LE), sensible heat flux (H) and soil heat flux (G), present seasonal behavior in the study area.

The net radiation, latent heat flux, and soil heat flux reach maximum values in the rainy season due to the higher amount of water vapor in the atmosphere and the greater amount of energy available in summer months.

Throughout the year the largest portion of net radiation in the study area is represented by the latent heat flux (LE), indicating that there is water availability for the evapotranspiration processes even in the drought season.

The raw data without calibration of MATMNXFLX and NOAH FLDAS products have tendencies of underestimation of latent heat flux and overestimation of sensible heat flux.

The adjustment regressions of the MATMNXFLX and FLDAS NOAH sensing products data present satisfactory results in latent heat flux estimates in the Mato-Grosso Pantanal.

## 5. ACKNOWLEDGMENT

The authors thank the National Council for Scientific and Technological Development (CNPQ) for the financial support through 407998/2016-0 "Study of the relationship between the variation of CO2 concentration and micrometeorological variables in the Mato Grosso Pantanal" 424915/2016-2 "Carbon Dynamics in the Mato Grosso Pantanal: Influence of efflux, flow, and CO2 stock", the Coordination of Improvement of Higher Level Personnel " (CAPES) together with the CNPq for the masters and doctorate scholarships awarded to the authors, and the Graduate Program in Environmental Physics (PPGFA) of the Federal University of Mato Grosso for encouraging research.

## 6. REFERENCES

ARAÚJO, A. L.; SILVA, M. T.; DA SILVA, B. B.; DOS SANTOS, C. A. C.; DO AMORIM, M. R. B. Modelagem Simplificada Para Estimativa do Balanço de Energia à Superfície em Escala Regional (R-SSEB). **Revista Brasileira de Meteorologia**, v. 32, n. 3, p. 433-446, 2017.

BASTABLE, H. G.; SHUTTLEWORTH, W. J.; DALLAROSA, R. L. G.; FISCH, G.; NOBRE, C. A. Observations of climate, albedo, and surface radiation over cleared and undisturbed Amazonian forest. **International Journal of Climatology**, Chichester -Inglaterra, v. 13, n. 7, p. 783-796, 1993.

BIUDES, M. S., CAMPELO JÚNIOR, J. H., NOGUEIRA, J. S.; SANCHES, L. Estimativa do balanço de energia em cambarazal e pastagem no norte do Pantanal pelo método da razão de Bowen. **Revista Brasileira de Meteorologia**, São José dos Campos, SP, v. 24. n. 2, p. 135-143, 2009.

BIUDES, M. S.; VOURLITIS, G. L.; MACHADO, N. G.; ARRUDA, P. H. Z.; NEVES, G. A. R.; LOBO, F. A.; NEALE, C. M.U.; NOGUEIRA, J. S. Patterns of energy Exchange for tropical ecosystems across a climate gradient in Mato Grosso, Brazil. **Agricultural and Forest Meteorology**, Amsterdam, v. 202, p. 112-124, 2015.

BLOOM, S.; DA SILVA, A.; DEE, D.; BOSILOVICH, M.; CHERN, J. D.; PAWSON, S.; SCHUBERT, S.; SIENKIEWICZ, M.; STAJNER, I.; TAN, W. W.; WU, M. L. Documentation and Validation of the Goddard Earth Observing System (GEOS) Data Assimilation System - Version 4, Technical Report Series on Global Modeling and Data Assimilation, 2005.

BOWEN, I. S. The ratio of heat losses by conductions and by evaporation from any water surface. Physical. **Review Serial**, v. 27, p. 779-787, 1926.

BURBA, G. G.; VERMA, S. B.; KIM, J. Surface energy fluxes of Phragmites australis in a prairie wetland. **Agricultural and forest meteorology**, Amsterdam, v. 94, n. 1, p. 31-51, 1999.

CURADO, L. F. A.; RODRIGUES, T. R.; BIUDES, M. S.; DE PAULO, S. R.; DE PAULO, I. J. C.; NOGUEIRA, J. S. Estimativa sazonal da emissividade atmosférica através da Equação de Brutsaert no norte do Pantanal Mato-grossense. **Ciência e Natura**, Santa Maria-RS, v. 33 n. 2, p. 167, 2011.

CURADO, L. F. A.; DE SOUZA NOGUEIRA, J.; SANCHES, L.; RODRIGUES, T. R.; DE ALMEIDA LOBO, F.; BÍUDES, M. S. Inter Seasonality of the Energy Fluxes in Brazilian Savana — Mato Grosso — Brazil. **Atmospheric and Climate Sciences**, v. 4, n. 2, p. 219-230, 2014.

DA SILVA, JOÃO DOS SANTOS VILA; DE MOURA ABDON, MYRIAN. Delimitação do Pantanal brasileiro e suas sub-regiões. **Pesquisa Agropecuária Brasileira**, Rio de Janeiro, RJ v. 33, n. 13, p. 1703-1711, 1998.

DA SILVA, L. B., NOVAIS, J. W. Z., SANCHES, L., MACHADO, N. G., AQUINO, A. M., & DA SILVA SALLO, F. (2018). Serrapilheira e Efluxo de Co2 do Solo em Floresta Sazonalmente Alagável no Pantanal Brasileiro**. Ensaios e Ciência: C. Biológicas, Agrárias e da Saúde**, v. 21, n. 3, p. 178-182, 2018.

EFRON, B.; TIBSHIRANI, R. J. **An introduction to the bootstrap**. Chapman & Hall, New York. p. 443, 1993.

FANTIN-CRUZ, I.; GIRARD, P.; ZEILHOFER, P.; COLLISCHONN, W.; NUNES DA CUNHA, C. Unidades fitofisionômicas em mesoescala no Pantanal Norte e suas relações com a geomorfologia. **Biota Neotropica**, v. 10, n. 2, p. 31-38, 2010.

FOLEY, J. A.; COSTA, M. H.; DELIRE. C.; RAMANKUTTY, N.; SNYDER, P. Green surprise? How terrestrial ecosystems could affect earth's climate**. Frontiers in Ecology and the Environment**, v. 1, n. 1, p.38-44, 2003.

GONÇALVES, J. B. **Calibração do modelo de superfície noah lsm: aplicação em uma região agrícola no sul do Brasil**. 2016. 109 f. Tese (Doutorado em Física) - Universidade Federal de Santa Maria, Santa Maria, 2016.

INSTITUTO BRASILEIRO DE GEOGRAFIA E ESTATÍSTICA - IBGE. **Mapa de Biomas do Brasil**; primeira aproximação. Rio de Janeiro: IBGE. 2004.

MACHADO, N. G.; SANCHES, L.; AQUINO, A. M.; SILVA, L. B.; NOVAIS, J. W. Z.; Biudes, M. S. Growth rhythm of *Vochysia divergens* Pohl (Vochysiaceae) in the Northern Pantanal. **Acta Scientiarum. Biological Sciences**, v. 37, n. 1, p.81-90, 2015.

MACHADO, N. G.; BIUDES, M. S.; ANGELINI, L. P.; DE SOUZA MÜTZENBERG, D. M.; NASSARDEN, D. C. S.; DE SOUZA BILIO, R.; NOGUEIRA, J. S. Sazonalidade do Balanço de Energia e Evapotranspiração em Área Arbustiva Alagável no Pantanal Mato-Grossense. **Revista Brasileira de Meteorologia**, v. 31, n.1, p. 82-91, 2016.

MCNALLY, A.; ARSENAULT, K.; KUMAR, S.; SHUKLA, S.; PETERSON, P.; WANG, S.; FUNK, C.; PETERS-LIDARD, C. D.; VERDIN, J. P. A land data assimilation system for sub-Saharan Africa food and water security applications. **Scientific data**, v. 4, p. 170012, 2017. DOI: https://doi.org/10.1038/sdata.2017.12

MEINZER, F. C.; GOLDSTEIN, G.; FRANCO, A. C.; BUSTAMANTE, M.; IGLER, E.; JACKSON, P.; RUNDEL, P. W. Atmospheric and hydraulic limitations on transpiration in Brazilian cerrado woody species. **Functional Ecology**, v. 13, n. 2, p. 273-282, 1999.

NUNES DA CUNHA, C.; JUNK, W. J. Distribution of woody plant communities along the flood gradient in the Pantanal of Poconé, Mato Grosso, Brazil. **International Journal of Ecology and Environmental Sciences**, v. 27, n. 2, p. 63-70, 2001.

PEREZ, P. J.; CASTELLVI, F.; IBAÑEZ, M.; ROSELL, J. I. Assessment of reliability of Bowen ratio method for partitioning fluxes. **Agricultural and Forest Meteorology**, v. 97, p.141-150, 1999.

QUERINO, C. A. S., BIUDES, M. S., MACHADO, N. G., DA SILVA QUERINO, J. K. A.; NETO, L. A. S.; DA SILVA, M. J. G.; NOGUEIRA, J. (2017). BALANÇO DE ONDAS CURTAS SOBRE FLORESTA SAZONALMENTE ALAGÁVEL DO PANTANAL MATO-GROSSENSE. **Revista Brasileira de Climatologia**, [S.I.] v.20, p.252-266.

RIENECKER, M. M.; SUAREZ, M. J.; GELARO, R.; TODLING, R.; BACMEISTER, J.; LIU, E.; BOSILOVICH, M. G.; SCHUBERT, S. D.; TAKACS, L.; KIM, G. K.; BLOOM, S.; CHEN, J.; COLLINS, D.; CONATY, A.; SILVA, A.; GU, W.; JOINER, J.; KOSTER, R. D.; LUCCHESI, R.; MOLOD, A.; OWENS, T.; PAWSON, S.; PEGION, P.; REDDER, C. R.; REICHLE, R.; ROBERTSON, F. R.; RUDDICK, A. G.; SIENKIEWICZ, M.; WOOLLEN, J. MERRA: NASA's modern-era retrospective analysis for research and applications. **Journal of climate**, v. 24, n. 14, p. 3624-3648, 2011. https://doi.org/10.1175/JCLI-D-11-00015.1

ROBERTS, J. B.; ROBERTSON, F. R.; CLAYSON, C. A.; BOSILOVICH, M. G. Characterization of turbulent latent and sensible heat flux exchange between the atmosphere and ocean in MERRA. **Journal of Climate**, v. 25, n. 3, p. 821-838, 2012. DOI: 10.1175/JCLI-D-11-00029.1

RODRIGUES, T. R.; CURADO, L. F. A.; NOVAIS, J. W. Z.; DE OLIVEIRA, A. G.; ROBERTO, S.; DE PAULO, M. S. B. E.; NOGUEIRA, J. D. S. Distribuição dos componentes do balanço de energia do Pantanal Mato-Grossense. **Revista de Ciências Agroambientais,** Alta Floresta, v. 9, n. 2, p.165-175, 2011.

RODRIGUES, T. R.; VOURLITIS, G. L.; LOBO, F. D. A.; OLIVEIRA, R. G.; NOGUEIRA, J. S. Seasonal variation in energy balance and canopy conductance for a tropical savanna ecosystem of south central Mato Grosso, Brazil. **Journal of Geophysical Research: Biogeosciences**, v. 119, n. 1, p. 1-13, 2014.

SANTOS, R. B.; DE SOUZA, A. P.; SILVA, A. C.; DE ALMEIDA, F. T.; ARANTES, K. R.; DE SIQUEIRA, J. L. Planejamento da pulverização de fungicidas em função das variáveis meteorológicas na região de Sinop – MT. **Global Science and Technology**, Rio Verde, v.6, n.1, p.72-88, jan./abr. 2013.

SOUZA, A. P. DE; MOTA, L. L. DA; ZAMADEI, T.; MARTIM, C. C.; ALMEIDA, F. T. DE; PAULINO, J. Classificação climática e balanço hídrico climatológico no estado de Mato Grosso. **Nativa**, Sinop, v. 1, n. 1, p. 34-43, 2013.

VAREJÃO-SILVA, M. A. **Meteorologia e climatologia**. Recife: Versão Digital, 2006. 463 p.

VERMA, S.B.; ROSENBERG, N.J.; BLAD, B.L. Turbulent exchange coefficients for sensible heat and water vapor under advective conditions. **Journal of Applied Meteorology**, Boston-MA, v.17, p. 330-338, 1978.